JOURNAL OF GEOPHYSICAL RESEARCH, VOL. 99, NO. C4, PAGES 7845–7850, APRIL 15, 1994

Deep water nutrient and oxygen gradients in a modern coastal upwelling zone and their paleoceanographic implications

Paul W. Jewell

Department of Geology and Geophysics, University of Utah, Salt Lake City

Abstract. Dissolved phosphate and oxygen data from the waters at >300 m depth beneath the Peru upwelling system imitate observed onshore/offshore surface productivity data. Positive onshore phosphate gradients and negative onshore oxygen gradients are greater in deeper water (up to 1000 m), reflecting the decreasing degree of horizontal mixing at depth. Mass balance reconstructions of surface productivity, nutrient remineralization, and onshore-offshore chemical gradients suggest that the lack of wide continental shelves during glacial climates would lead to more pronounced dissolved nutrient and oxygen gradients in the deep water adjacent to continental margins. Horizontal $\delta^{13}C$ gradients in sediments beneath highly productive coastal upwelling zones may have been as high as 0.5–1.0‰ per 100 km, suggesting caution in the interpretation of benthic $\delta^{13}C$ samples adjacent to continental margins during low sea level stands.

Introduction

Coastal upwelling zones form a critical link in the overall biogeochemical cycles of the ocean. In the modern ocean, photosynthesis consumes nutrients and produces oxygen in the photic zone. Sinking and subsequent degradation of organic matter causes deep-ocean water to be enriched in nutrients and depleted in oxygen. These nutrient-rich waters are brought to the surface by Ekman pumping at equatorial latitudes, Ekman transport along the eastern edges of ocean basins, and convective mixing of surface and deep waters at high latitudes. Differing global climates appear to have altered some of these processes. For instance, it is widely believed that the dissolved, inorganic $\delta^{13}C$ of deep-ocean water was approximately 0.5‰ lighter during the last glacial maximum [e.g., *Curry et al.*, 1988; *Duplessy et al.*, 1988; *Sarnthein et al.*, 1988] and that this change is related to increased inputs of isotopically light organic carbon. A number of authors have suggested that at least part of the glacial decrease in $\delta^{13}C$ is related to increased productivity in coastal upwelling zones [*Newell et al.*, 1978; *Berger and Keir*, 1984; *Boyle*, 1986; *Sarnthein et al.*, 1988].

It has long been recognized that coastal upwelling zones contain some of the most biologically productive surface waters in the ocean. The most productive waters are located adjacent to the coast [*Huntsman and Barber*, 1977; *Packard et al.*, 1983]. Waters further offshore [50–200 km] are less productive than the nearshore waters, although the productivity is still significantly higher than that of the open ocean [e.g., *Suess et al.*, 1987; *Berger*, 1989].

It is logical to expect that dissolved nutrients and oxygen in deep waters beneath upwelling zones would reflect the onshore-offshore surface productivity gradients. In the absence of onshore-offshore mixing processes, the dissolved chemical components should imitate surface productivity. On the other hand, very strong mixing should result in small or variable deep-water chemical gradients.

The relative importance of surface productivity gradients, deep-water nutrient chemistry, and the strength of onshore-offshore mixing is considered here through the detailed examination of data from the Peru upwelling system. Results are then considered in the light of hypothesized increased coastal upwelling and differing shelf bathymetry of glacial climates.

Paper number 94JC00088.
0148-0227/94/94JC-00088$05.00

Onshore-Offshore Chemical Gradients

Several criteria were considered in selecting a data set for studying deep water (>300 m) mixing and geochemistry in coastal upwelling zones. The locus of many coastal upwelling zones in the modern ocean is over relatively shallow water [e.g., northwest Africa, southwest Africa], thus making it difficult to observe changes in nutrient chemistry with depth. Finally, the chemical, physical, and biological variability of upwelling zones in both time and space is well documented [e.g., *Small and Menzies*, 1981; *Barber and Smith*, 1981; *Chavez et al.*, 1991].

The portion of the Coastal Upwelling Ecosystem Analysis JOINT-II experiment (hereafter referred to as JOINT-II) data set collected at 15°S off the coast of Peru during March–May, 1977 represented the most suitable data for this study (Figure 1). The continental shelf is relatively narrow at this location, thereby permitting the examination of deep-water chemistry. Longshore currents beneath the well-documented poleward undercurrent (>300 m) are relatively slow [*Brockman et al.*, 1980; *Brink et al.*, 1980]. A number of transects at 15°S were conducted over the 3-month period of the project. Time-integrated summaries of surface productivity [*Packard et al.*, 1983] (Figure 2) as well as physical parameters [*Smith*, 1981] over this time period are reported.

Water between 300 and 1000 m at 15°S is composed of Eastern South Pacific Intermediate Water (ESPIW) which has a high-latitude, low-salinity origin [*Reid*, 1973; *Emery and Meincke*, 1986]. ESPIW is a well-defined water mass south of 12°S [*Reid*, 1973]. Mixing of two distinct, intermediate-depth water masses with differing chemical properties

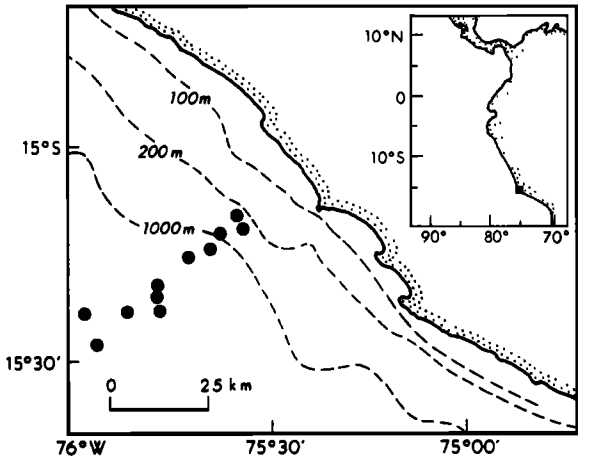

Figure 1. Location of samples from the JOINT-II project used in this study [*Hafferty et al.*, 1978].

is unlikely at 15°S, particularly over the <100 km horizontal distances considered in this study.

Dissolved phosphate and oxygen were the elements considered in greatest detail in the deep Peru waters. Nitrate reduction to nitrite and presumably to N_2 is relatively common in the upper portion (<400 m) of the Peru upwelling system [*Hafferty et al.*, 1978; *Codispoti*, 1983]. Even small amounts of nitrate reduction at greater depths could mask subtle nutrient gradients, and therefore nitrate was not considered in this analysis.

Onshore-offshore mixing processes are very important in analyzing onshore-offshore chemical gradients. The nature of these mixing processes is ambiguous. Advection clearly plays an important role, although mixing along isopycnal surfaces in a manner similar to that proposed for the open ocean [*Okubo*, 1971; *Pingree*, 1972; *Jenkyns*, 1991] may also be a factor. At depths between 150 and 400 m, isopycnal surfaces within 100 km of the Peru coast during the JOINT-II project warp downward close to shore [e.g., *Codispoti*, 1983]. Isopycnal surfaces below 400 m depth showed only minor horizontal variation (Figure 3). Onshore-offshore chemical variations of the JOINT-II data at >400 m depth could therefore be studied using either constant depth or constant density. Constant depth is used in this study.

Within the JOINT-II data set a specific series of stations that were occupied over a relatively short period of time in a direction perpendicular to the shore were selected (Figure 1). Along each of these transects, phosphorous and oxygen concentrations were recorded at specific depths. Concentration gradients were obtained from regression of oxygen or phosphate data with offshore distance (e.g., Figure 4). Concentration gradients and correlation coefficients are summarized in Table 1.

Results

Calculated onshore-offshore phosphate gradients range from −0.16 to 0.86 μmol/L/100 km. Three of the four

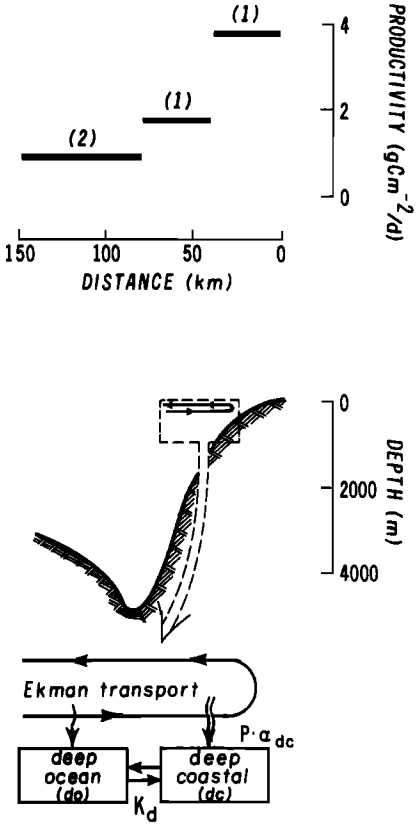

Figure 2. Cross-shelf bathymetry and summary of published time averaged surface productivity. Lines labeled 1 are from *Packard et al.* [1983]; line labeled 2 is from *Suess et al.* [1987]. Box model representation is shown below the idealized bathymetry.

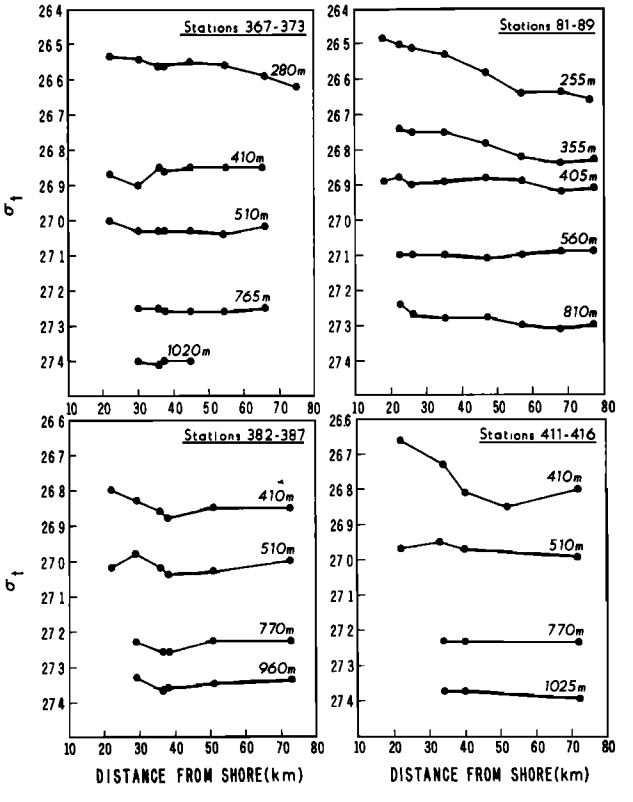

Figure 3. Onshore-offshore density variations at various depths of the JOINT-II data set (from *Hafferty et al.* [1978]). Transects which showed greater than 0.1 σ_t variation over the transect distance were not included in Figures 5 and 6 and Table 1.

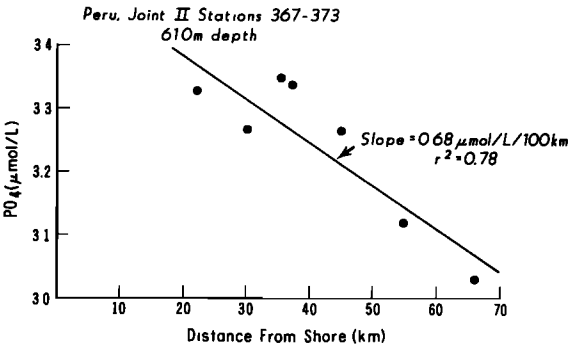

Figure 4. Phosphate concentration versus offshore distance for 610 m depth, stations 367–373, JOINT-II data set. Plots such as this make up the individual points shown in Figures 3 and 4, and Table 1.

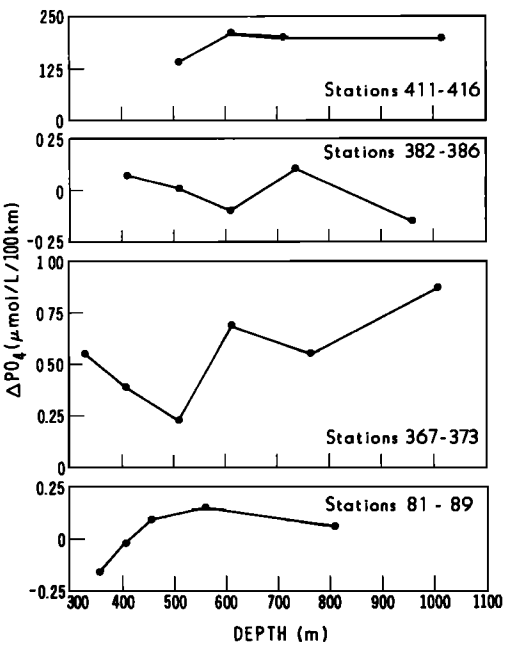

Figure 5. Plots of onshore-offshore phosphate gradients as a function of depth for various transects at 15°S in the Peru upwelling system.

transects from the JOINT-II project show shoreward increases in phosphate gradients (Figure 5). In general, higher correlation coefficients of the phosphate data with offshore distance are associated with the largest phosphate gradients (Table 1). The greatest gradients also occur at the greatest depths. Smaller absolute values of the gradients (either negative or positive) are most common in shallower water.

All four oxygen profiles show onshore-offshore oxygen gradients which become more negative with depth (Table 1; Figure 6). At <700 m depth, oxygen gradients range from −7.4 to 15.6 μmol/L/100 km, while at greater depths the gradients are −16.3 to 7.3. Note that the ratios of oxygen and phosphate gradients do not follow a Redfield stoichiometry. This may be the result of nitrate reduction, which would tend to make the oxygen gradients relatively smaller.

The increasing magnitude of phosphate gradients and decrease in oxygen gradients with depth can be explained within the context of current data from the Peru system (Table 2). Although net onshore-offshore velocities in the Peru system are very close to zero, standard deviations are larger (up to 5 cm/s) and consistently decrease with depth. The increase in onshore-offshore chemical gradients with depth is probably related to dynamic features such as strength of poleward undercurrents (the Peru-Chile undercurrent in this case) and associated coastal trapped waves.

Table 1. Summary of Onshore-Offshore Phosphate and Oxygen Gradients at 15°S

Stations	Dates	Transect Length, km	Depth, m	ΔPO_4, μmol/L/ 100 km	Phosphate r^2	ΔO_2, μmol/L/ 100 km	Oxygen r^2
81–89	March 18–19, 1977	55	355	−0.16	0.32		
			405	−0.03	0.04		
			455	0.09	0.68	10.1	0.32
			560	0.15	0.53	9.6	0.32
			810	0.06		−16.3	0.72
367–373	May 5, 1977	44	330	0.53	0.78		
			410	0.39	0.75		
			510	0.24	0.69	15.6	0.55
			610	0.68	0.78	0.3	0.02
			765	0.54	0.89	7.3	0.51
			1,020	0.86	0.91	−13.2	0.41
382–387	May 8–9, 1977	51	410	0.07	0.16		
			510	0.01	0	6	0.21
			610	−0.11	0.25	10.8	0.84
			765	0.1	0.37	1.3	0.08
			960	−0.14	0.91	−3.1	0.13
411–416	May 13, 1977	50	510	0.14	0.21	−7.4	0.72
			610	0.21	0.5	2.1	0.21
			770	0.2	0.4	−10.5	0.72
			1,025	0.2	0.34	−8.3	0.9

Data are from *Hafferty et al.* [1978].

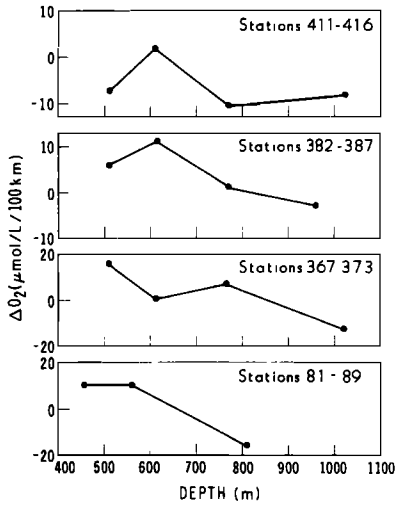

Figure 6. Plots of onshore-offshore oxygen gradients as a function of depth for various transects at 15°S in the Peru upwelling system.

These features have been observed over shelf breaks in many coastal settings as well as in model studies [e.g., *Smith*, 1981; *Philander and Yoon*, 1982]. Poleward undercurrents are most intense at depths from 50–300 m and less significant at depths of 500–1000 m. Onshore-offshore mixing is therefore smaller, and nutrient concentration gradients are larger at these greater depths.

Mass Balance Calculations

The relationship between surface productivity, onshore-offshore mixing, and chemical gradients can be determined through simple mass balance relationships.

$$(PO_{4,dc} - PO_{4,do})K_d = (P_{dc} - P_{do})\alpha_{dc} \quad (1)$$

$$(O_{2,dc} - O_{2,do})K_d = -r(P_{dc} - P_{do})\alpha_{dc} \quad (2)$$

K_d is the onshore-offshore mixing, P is surface productivity, α is the fraction of surface productivity remineralized in a given subsurface box, and r is the ratio of oxygen to phosphorous. K_d contains the units of volume flux per unit length of shoreline, that is, square meters per second. The subscripts *dc* and *do* represent the deep coastal and deep ocean boxes (Figure 2), respectively. The spatial separation of the *dc* and *do* boxes (Figure 2) means that the concentration terms on the left-hand sides of (1) and (2) represent a horizontal concentration gradient. Multiplying oxygen and phosphorous concentrations (units of micromoles per liter or millimoles per cubic meter) by the mixing rates (square meter per second) in the left-hand sides of (1) and (2) gives a mass flux per unit length of shoreline (moles per second per meter).

Box model primary productivity, P on the right-hand sides of (1) and (2), has units of moles per meter per second and must be converted to values commonly reported for surface productivity (usually g C m^{-2}/yr). Assuming a C:PO_4 of 106, it can be found that 1 g C m^{-2} yr^{-1} = 2.5 × 10^{-8} mmol P m^{-2}/s. A PO_4:O_2 of −170 [*Takahashi et al.*, 1985] is used to represent r in (2). Multiplying these values by the transect width (approximately 50 km; Table 1) gives the appropriate units for P.

The fraction of surface productivity remineralized in the *dc* box (α_{dc}) is obviously dependent on the thickness of the *dc* and *do* boxes. In the model presented here this thickness is arbitrary. In the calculations presented below the boxes are 100 m thick. In other words, the mass balance model is actually a series of boxes of equal thickness (Figure 2).

Approximations for K_d can be found by assuming values of α_{dc}, and applying the productivity and deep-water phosphate and oxygen data presented above (Table 1; Figures 5 and 6). Relationships between organic carbon flux and depth have been discussed by numerous researchers. For intermediate depth water, approximately 1% of sinking organic matter is remineralized for every 100 m of depth [e.g., *Berger et al.*, 1989]. Since the model deep-water boxes are thin (100 m) and relatively wide (50 km), the only flux of constituents from the sediments would be laterally into the *dc* box. It is assumed that remineralization of sinking organic matter is a much greater source of dissolved chemical components than lateral input from the sediments. With these assumptions, K_d values for the Peru system would range between 0.03 m^2/s for deep water to >0.30 m^2/s for shallow water using the phosphate gradient data (Figure 7a). Oxygen gradient data give a deep-water K_d of approximately 0.16 m^2/s, with much higher values in shallow water. It is important to emphasize that these absolute values are crude estimates. Relative changes in K_d are as diagnostic as actual values, and it is these changes as well as onshore-offshore productivity gradients that determine the onshore-offshore chemical gradients in (1) and (2).

In seawater, oxidants are consumed in the order $O_2 \rightarrow NO_3^- \rightarrow Mn^{4+} \rightarrow Fe^{3+} \rightarrow SO_4^{2-}$ [*Stumm and Morgan*, 1981]. Since the amount of dissolved Mn^{4+} and Fe^{3+} in the ocean is small, the primary oxidants are oxygen, nitrate, and sulfate. In the deep portion of upwelling zones, oxygen, and more rarely, nitrate are consumed.

The box model calculations can be used to illustrate the general controls of available oxidants (i.e., oxygen, nitrate, and sulfate) in the deep coastal zone of upwelling system. Here it is assumed that "oxygen" concentrations of 0 to −30 μmol/L represent nitrate reduction and concentrations below −30 μmol/L represent sulfate reduction. In reality this is only a generalization because it neglects the fact that nitrate reduction occurs before oxygen is completely depleted as well as neglects the formation of nitrite (NO_2^-) and other

Table 2. Summary of Onshore-Offshore Velocities at 15° S in the Peru Upwelling System

Depth, m	Latitude	Longitude	Onshore-Offshore Velocity, cm/s
197	5° 01′	81° 31′	1.5 ± 4.0
560			−0.3 ± 3.6
860			−0.3 ± 1.9
195	5° 00′	81° 44′	0.0 ± 6.2
235			0.0 ± 4.2
415			−2.1 ± 4.0
183	15° 11′	75° 34′	−0.3 ± 3.4
283			−0.2 ± 2.1
115	15° 10′	75° 36′	−1.1 ± 4.7
214			−0.3 ± 3.1
512			0.9 ± 1.6

Data are from *Brockmann et al.* [1980].

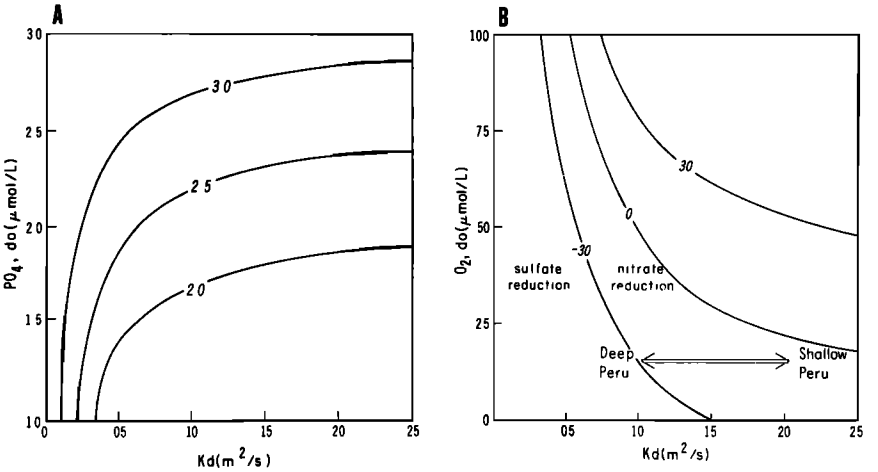

Figure 7. (a) Phosphate concentrations (μmol/L) and (b) oxygen concentrations (μmols/L) in the deep coastal (*dc*) box as a function of deep ocean (*do*) concentration and onshore-offshore mixing rates (K_d). Differences between *do* and *dc* concentrations represent the horizontal gradients expressed in Equations (1) and (2) of the text.

intermediate chemical species. For the sake of a simplified examination of oxidant consumption, however, this simplification is justified. With this assumption, it is interesting to note that nitrate- and sulfate-reducing water would be common at very low onshore-offshore mixing rates regardless of the oxygen content of the water which feeds into it (Figure 7b). In other words, the only way an oxidant can be exchanged between the deep ocean and the deep coastal zone is by onshore-offshore mixing (Figure 2). If this mixing rate is low, very high concentration gradients will result.

It is very difficult to produce quantitative estimates of either paleonutrient or paleo-oxygen concentrations. A much more effective tracer of deep water chemistry is $\delta^{13}C$, which is routinely measured in the tests of benthic foraminifera. Previous studies have shown a close correspondence between $\delta^{13}C$ of dissolved inorganic carbon and oxygen utilization in the world ocean [e.g., *Kroopnick*, 1985].

A mass balance relationship for $\delta^{13}C$ can be constructed by balancing total CO_2 in a fashion similar to that of (1) and (2). All terms in the equation are then multiplied by appropriate values of per mill $\delta^{13}C$ (i.e., $-21‰$ for marine organic matter). Assuming that the total CO_2 of the deep water is not significantly altered by downward particle flux, then the mass balance relationship for the deep-coastal box along the sediment water interface becomes

$$\delta^{13}C_{,dc} - \delta^{13}C_{,do} \equiv \Delta\delta^{13}C = \frac{(P_{dc} - P_{do})\alpha_s}{K_d} \quad (3)$$

Most organic carbon which reaches the seafloor is remineralized at the sediment-water interface. The numerator on the right-hand side of the equation is thus assumed to represent a net onshore-offshore gradient of carbon flux. A plot of (3) demonstrates that significant horizontal $\delta^{13}C$ gradients (up to 1‰) are possible when onshore-offshore mixing is low (Figure 8).

Discussion

Regressive sea levels during glacial climates would cause the most productive portions of upwelling zones to overlay relatively deep water. Various paleoceanographic studies have also suggested that increased zonal wind strength during glacial times would cause these coastal upwelling zones to be more productive than modern upwelling zones [e.g., *Sarnthein et al.*, 1988]. Significant onshore-offshore gradients of $\delta^{13}C$ in benthic waters would thus be expected in these situations because the cross-shelf gradients of organic carbon flux would be relatively high and the degree of onshore-offshore mixing in the deep waters would be relatively low. For instance, assume that the onshore-offshore productivity difference observed in the innermost 50 km of the Peru system (approximately 700 gC m^{-2}/yr) were over the glacial period bathymetry of northwest Africa. At this location, depths of approximately 2000 m are present within 50 km of the glacial shoreline. The onshore-offshore $\delta^{13}C$ gradient would have been 0.7‰, assuming the remineralization relationships of *Berger et al.* [1989] and the low deep-water mixing rates calculated previously.

In reconstructing the chemical oceanography of the last glacial maximum, considerable attention has been placed on the vertical gradients of properties. For reconstructing these vertical gradients, $\delta^{13}C$ in planktonic and benthic foraminifera is particularly useful [e.g., *Curry et al.*, 1988; *Duplessy et al.*, 1988; *Sarnthein et al.*, 1988]. It is generally believed that the dissolved inorganic carbon of deep water was at least 0.5‰ lighter during the last glacial maximum, although considerable variability exists within specific ocean basins [*Sarnthein et al.*, 1988].

Results of the mass balance calculations presented here suggest that horizontal $\delta^{13}C$ gradients adjacent to continental margins can be as significant as the documented vertical $\delta^{13}C$ gradients in the open ocean (Figure 8). Benthic $\delta^{13}C$ data from cores within 100 km of the modern 100 m isobath of productive continental margins should be considered within the context of the results of the data and simple model presented here. Examples of published $\delta^{13}C$ analyses where this effect might have been operative include cores adjacent to northwest Africa between 17° and 23°N. [e.g., *Sarnthein et al.*, 1988] and Ocean Drilling Program sites 723–726 in the Arabian Sea [*Prell et al.*, 1991].

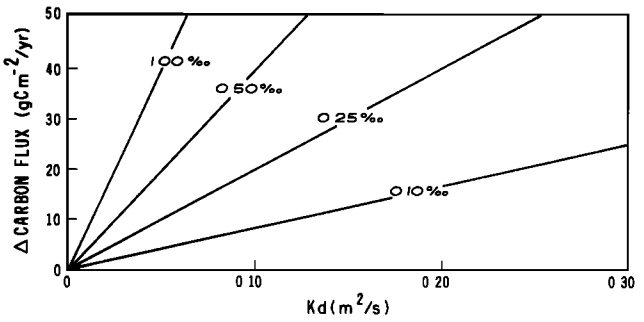

Figure 8. Onshore-offshore $\Delta\delta^{13}C$ gradients plotted as a function of onshore-offshore mixing and onshore-offshore organic carbon flux differences.

Acknowledgments. Lou Codispoti provided copies of the JOINT-II data. Robbie Toggweiler clarified my thinking about the mechanisms of cross-shelf mixing. Comments by Kent Fanning and two anonymous reviewers improved the manuscript. Acknowledgment is made to the donors of The Petroleum Research Fund, administered by the American Chemical Society for support of this research.

References

Barber, R. T., and R. L. Smith, Coastal upwelling ecosystems, in *Analysis of Marine Ecosystems*, edited by A. R. Longhurst, pp. 31–68, Academic, San Diego, Calif., 1981.

Berger, W. H., Global maps of ocean productivity, in *Productivity in the Ocean: Present and Past: Dahlem Workshop Reports, Life Sciences Research Report 44*, edited by W. H. Berger, V. S. Smetacek, and G. Wefer, pp. 429–454, John Wiley, New York, 1989.

Berger, W. H., and R. S. Keir, Glacial-Holocene changes in atmospheric CO_2 and the deep-sea record, in *Climate Processes and Climate Sensitivity*, *Geophys. Monogr. Ser.*, vol. 29, edited by J. E. Hansen and T. Takahashi, pp. 337–351, AGU, Washington, D. C., 1984.

Berger, W. H., V. S. Smetacek, and G. Wefer, Ocean productivity and paleoproductivity—An overview, in *Productivity in the Ocean: Present and Past: Dahlem Workshop Reports, Life Sciences Research Report 44*, edited by W. H. Berger, V. S. Smetacek, and G. Wefer, pp. 1–34, John Wiley, New York, 1989.

Boyle, E. A., Deep Ocean circulation, preformed nutrients, and atmospheric carbon dioxide: Theories and evidence from oceanic sediments, in *Mesozoic and Cenozoic oceans*, in *Geodyn. Ser.*, vol. 15, edited by K. J. Hsu, pp. 49–59, AGU, Washington, D. C., 1986.

Brink, K. H., D. Halpern, and R. L. Smith, Circulation in the Peruvian upwelling system near 15°S, *J. Geophys. Res.*, *85*, 4036–4048, 1980.

Brockmann, C., E. Fahrbach, A. Huyer, and R. L. Smith, The poleward undercurrent along the Peru coast: 5 to 15°S, *Deep Sea Res.*, *27A*, 847–856, 1980.

Chavez, F. P., R. T. Barber, P. M. Kosro, A. Huyer, S. R. Ramp, T. P. Stanton, and B. R. de Mendiola, Horizontal transport and the distribution of nutrients in the coastal transition zone off northern California: Effects on primary production, phytoplankton biomass, and species composition, *J. Geophys. Res.*, *96*, 14,833–14,848, 1991.

Codispoti, L. A., On nutrient variability and sediments in upwelling regions, in *Coastal Upwelling: Its Sedimentary Record, Part A: Responses of the Sedimentary Regime to Present Coastal Upwelling*, edited by E. Suess and J. Thiede, pp. 125–145, Plenum, New York, 1983.

Curry, W. B., J. C. Duplessy, and L. D. Labeyrie, Changes in the distribution of $\delta^{13}C$ of deep water total CO_2 between the last glaciation and the Holocene, *Paleoceanography*, *3*, 317–341, 1988.

Duplessy, J. C., N. J. Shackleton, R. G. Fairbanks, L. Labeyrie, D. Oppo, and N. Kallel, Deep water source variations during the last climatic cycle and their impact on the global deep water circulation, *Paleoceanography*, *3*, 343–360, 1988.

Emery, W. J., and J. Meincke, Global water masses: Summary and review, *Oceanol. Acta*, *9*, 383–391, 1986.

Hafferty, A. J., L. A. Codispoti, and A. Huyer, JOINT-II, R/V *Melville* Legs I, II, and IV; R/V *Iselin* Leg II bottle data, March–May, 1977, *Data Rep. 45*, 779 pp., Dept. of Oceanogr., Univ. of Washington, Seattle, 1978.

Huntsman, S. A., and R. T. Barber, Primary production off northwest Africa: The relationship to wind and nutrient conditions, *Deep Sea Res.*, *24*, 25–33, 1977.

Jenkyns, W. J., Determination of isopycnal diffusivity in the Sargasso Sea, *J. Phys. Oceanogr.*, *21*, 1058–1061, 1991.

Kroopnick, P. M., The distribution of ΣCO_2 in the world oceans, *Deep Sea Res.*, *32*, 57–84, 1985.

Newell, R. E., A. R. Navato, and J. Hsuing, Long-term global sea surface temperature fluctuations and their possible influence on atmospheric CO_2 concentrations, *Pure Appl. Geophys.*, *116*, 351–371, 1978.

Okubo, A., Ocean diffusion diagrams, *Deep Sea Res.*, *18*, 789–802, 1971.

Packard, T. T., P. C. Garfield, and L. A. Codispoti, Oxygen consumption and denitrification below the Peruvian upwelling, in *Coastal Upwelling: Its Sedimentary Record, Part A: Responses of the Sedimentary Regime to Present Coastal Upwelling*, edited by E. Suess and J. Thiede, pp. 147–173, Plenum, New York, 1983.

Philander, S. G. H., and J.-H. Yoon, Eastern boundary currents and coastal upwelling, *J. Phys. Oceanogr.*, *12*, 863–879, 1982.

Pingree, R. D., Mixing in the deep stratified ocean, *Deep Sea Res.*, *19*, 549–561, 1972.

Prell, W. L., et al., *Proc. Ocean Drill. Program Sci. Results*, *117*, 1991.

Reid, J. L., The shallow salinity minima of the Pacific Ocean, *Deep Sea Res.*, *20*, 51–68, 1973.

Sarnthein, M., K. Winn, J.-C. Duplessy, and M. R. Fontugne, Global variations of surface ocean productivity in low and mid latitudes: Influence on CO_2 reservoirs of the deep ocean and atmosphere during the last 21,000 years, *Paleoceanography*, *3*, 361–399, 1988.

Small, L. F., and D. W. Menzies, Patterns of primary productivity and biomass in a coastal upwelling region, *Deep Sea Res.*, *28A*, 123–149, 1981.

Smith, R. L., Descriptions and comparisons of specific upwelling systems, in *Coastal Upwelling Systems*, *Coastal and Estuarine Sciences*, vol. 1, edited by F. A. Richards, pp. 107–118, AGU, Washington, D. C., 1981.

Stumm, W., and J. J. Morgan, *Aquatic Chemistry*, 780 pp., John Wiley, New York, 1981.

Suess, E., L. D. Kulm, and J. S. Killingley, Coastal upwelling and a history of organic-rich mudstone deposition off Peru, in Marine Petroleum Source Rocks, edited by J. Brooks, and A. J. Fleet, pp. 181–197, *Spec. Publ. Geol. Soc.*, London, 1987.

Takahashi, T., W. S. Broecker, and S. Langer, Redfield ratio based in chemical data from isopycnal surfaces, *J. Geophys. Res.*, *90*, 6907–6924, 1985.

P. W. Jewell, Department of Geology and Geophysics, University of Utah, 717 W. C. Browning Building, Salt Lake City, UT 84112-1183.

(Received August 20, 1993; revised October 4, 1993; accepted December 29, 1993.)